World Journal of Management Science
Print ISSN: 2959-9628
Online ISSN: 2959-9636
DOI: https://doi.org/10.61784/wms3099

THE PREDICTION OF METEOROLOGICAL AND PHENOLOGICAL TRENDS AND ROUTE DECISION-MAKING DURING THE QINGMING FESTIVAL BASED ON ARIMA AND RANDOM FOREST REGRESSION

YiHan Ma
School of Business, Xi'an International Studies University, Xi'an, 710128, Shaanxi, China.

Abstract: Addressing the significant challenges in cultural tourism decision-making caused by unpredictable weather and uncertain flowering periods during the Qingming Festival, this study establishes a robust quantitative framework integrating meteorological forecasting, phenological prediction, and route optimization. Specifically, an ARIMA model is constructed to define "continuous drizzle" quantitatively and forecast precipitation probabilities for seven target cities. Concurrently, a Random Forest Regression model is introduced to accurately predict the onset and duration of flowering for cherry blossoms, peonies, and rapeseed flowers. Feature importance analysis reveals temperature as the dominant driver for cherry blossoms (weight 62.3%), with the model achieving a high goodness-of-fit of 0.91. Furthermore, a multi-objective planning model is developed using integer linear programming, generating an optimal closed-loop tour route connecting Wuhan, Xi'an, Luoyang, and Hangzhou. This route effectively balances flower-viewing experiences with rain-avoidance preferences while minimizing travel costs. The research innovates by establishing quantitative meteorological criteria and successfully transforming natural law predictions into personalized tourism decision-making strategies, providing valuable theoretical support and practical guidelines for smart cultural tourism in complex environments.
Keywords: ARIMA model; Random Forest; Multi-objective optimization

1 INTRODUCTION

The Qingming Festival is a major traditional spring festival in China, whose distinctive meteorological landscapes and floral blooming processes together constitute unique cultural significance and tourism value. However, the persistent drizzle caused by the convergence of cold and warm air masses, coupled with the sensitivity of flowering periods to meteorological factors, makes flower-viewing activities fraught with uncertainty. Previous research has largely focused on macro-level qualitative descriptions or single meteorological statistics, making it difficult to achieve coupled predictions of meteorological phenomena and plant phenology at the micro-urban scale. The innovation of this section lies in establishing quantitative criteria for identifying the "drizzling rain" weather phenomenon and utilizing machine learning algorithms to uncover the nonlinear driving patterns of multidimensional meteorological features on the growth and development of typical flowers [1,2]. Furthermore, through multi-objective optimization algorithms, we have achieved the transformation of research outcomes from natural law prediction to personalized tourism decision-making. The general research approach for this section is as follows: First, an ARIMA model is constructed based on historical precipitation probability sequences; through differencing and parameter identification, precipitation trends for the target city are predicted. Second, historical phenological observations and meteorological records are integrated, and a random forest regression model is trained using bootstrap sampling to quantify the explanatory power of meteorological factors on the onset of flowering and to infer future flowering windows. Finally, the meteorological and phenological prediction results are used as environmental constraints. Parameters such as flower-viewing priority and rain-avoidance sensitivity are set to construct a multi-objective decision-making model and calculate the optimal spatiotemporal tour routes [3-5].

2 PREDICTION MODEL OF "CONTINUOUS DRIZZLE" WEATHER DURING QINGMING FESTIVAL BASED ON ARIMA

2.1 Model Establishment

According to the *Classification Standards for Weather Phenomena* and the classification of the China Meteorological Administration, the daily rainfall classification standards are shown in Table 1. Daily precipitation between 0.1 mm and 9.9 mm is regarded as light rain. Combining the poetic and practical perspectives with the continuous feature of "continuous drizzle", the consecutive rainfall days shall be no less than two days. Therefore, the research standard for "continuous drizzle" in this study is set as follows:
Daily rainfall: $0.1 \leq P_t \leq 9.9$ (unit: mm)
Consecutive rainfall days: no less than two days.

Rainfall Classification Standards is shown in Table 1.

Table 1 Rainfall Classification Standards

Level	Daily Rainfall (mm)
Light rain	0.1~9.9
Moderate rain	10~24.9
Heavy rain	25~49.9

Let P_t denote the rainfall on day t, and the discriminant function is defined as:

$$S_t=\begin{cases}1, & 0.1\le P_t\le 9.9\\ 0, & \text{else}\end{cases} \tag{1}$$

Let the Qingming Festival window be $[t_1,t_2]$, and the continuous identification variable is defined as:

$$Q=\sum_{t=t_1}^{t_2} S_t \tag{2}$$

If $Q\ge 2$, it is considered that "continuous drizzle" occurs in the city during the Qingming Festival of that year [6,7].

The three core components of the ARIMA model are Auto-Regression (AR), Integration (I), and Moving Average (MA). The model is constructed through the following steps:

Test the stationarity of the time series: Before applying the ARIMA model, the primary task is to test the stationarity of the time series, which can be judged by plotting the time series and conducting the unit root test.

Differencing processing: If the time series is non-stationary, differencing processing is required to achieve stationarity, aiming to remove the trend and seasonal components in the time series.

Determine the parameters (p, d, q) of the ARIMA model:

p (order of auto-regression terms): determined by the Partial Auto-Correlation Function (PACF) plot.

d (number of differencing): determined by making the series stationary. The first-order differencing formula is:

$$y_t'=y_t-y_{t-1} \tag{3}$$

q (order of moving average terms): determined by the Auto-Correlation Function (ACF) plot.

Construct and fit the model: Use the selected parameters p, d, and q to construct the ARIMA model and fit the data, usually involving Maximum Likelihood Estimation (MLE) to estimate the model parameters.

Thus, the formula of the ARIMA model is as follows:

$$y_t=c+\phi_1 y_{t-1}+\phi_2 y_{t-2}+\cdots+\phi_p y_{t-p}+\varepsilon_t+\beta_1\varepsilon_{t-1}+\beta_2\varepsilon_{t-2}+\cdots+\beta_q\varepsilon_{t-q} \tag{4}$$

where y_t represents the value at current time t, ϕ_p represents the auto-regression coefficient, ε_t represents the white noise error term, and β_q is the moving average coefficient.

2.2 Model Solution

Step 1 Data Preprocessing and Stationarity Test

Data source: Based on the historical rainfall probability of cities during the Qingming Festival (2005-2024) in the chart, extract the rainfall probability time series of Xi'an, Turpan, Wuyuan, Hangzhou, Bijie, Wuhan, and Luoyang.

Stationarity test:

Plot the time series plots of rainfall probability for each city and observe the trend and seasonality.

Use the ADF unit root test; if the p-value > 0.05, the series is non-stationary and requires differencing. For example:

The original series of Xi'an may show a slight downward trend (requires first-order differencing).

The rainfall probability of Turpan is stable at a low level for a long time (may not require differencing).

Step 2 Parameter Determination and Model Fitting

Auto-Correlation Function (ACF) and Partial Auto-Correlation Function (PACF) analysis:

Xi'an: ACF tails off, PACF cuts off at lag 1 → significant AR(1) component.

Turpan: Neither ACF nor PACF shows significant cut-off → may be suitable for a simple MA model.

Differencing order (d): Most cities achieve stationarity through first-order differencing.

Model selection:

Xi'an: ARIMA(1,1,0) (based on PACF cut-off).

Turpan: ARIMA(0,0,1) (no obvious auto-regression trend).

Parameters for other cities are determined by similar methods.

Step 3 Model Diagnosis

Residual test:

Ljung-Box test to check whether the residuals are white noise (passed if p-value > 0.05).

Residual plots should show no auto-correlation and heteroscedasticity.

Historical Rainfall Conditions of Cities During the Qingming Festival (2005-2024) is shown in Figure 1. 5-year Moving Average Rainfall Trend is shown in Figure 2. City Percentage Heat Map is shown in Figure 3. City Percentage Radar Chart is shown in Figure 4 [8,9].

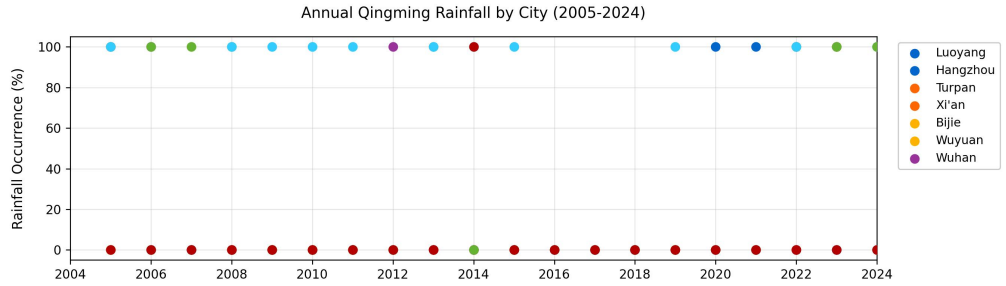

Figure 1 Historical Rainfall Conditions of Cities During the Qingming Festival (2005-2024)

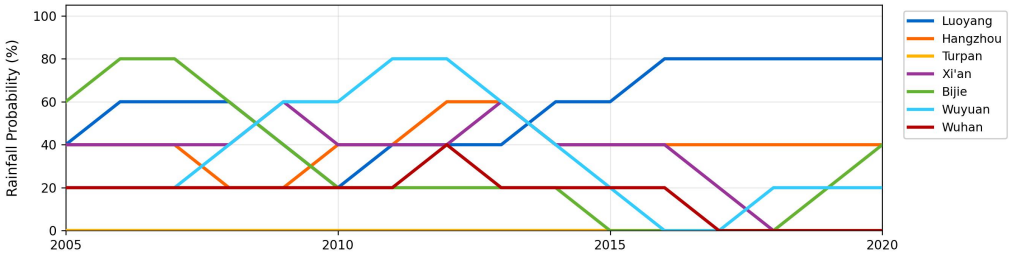

Figure 2 5-year Moving Average Rainfall Trend

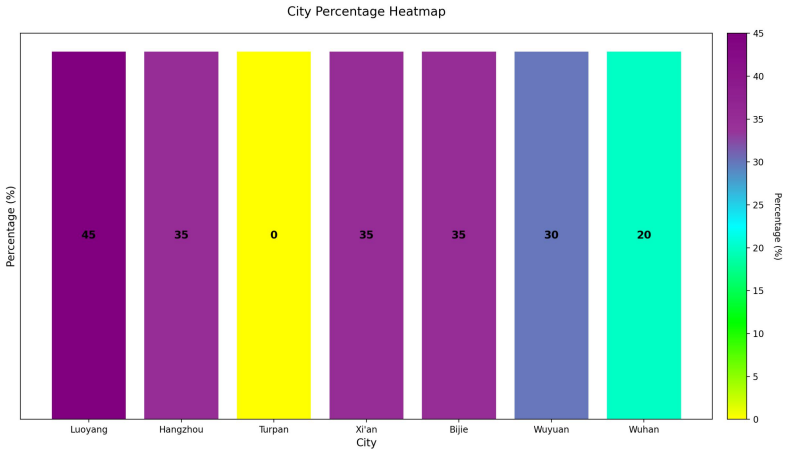

Figure 3 City Percentage Heat Map

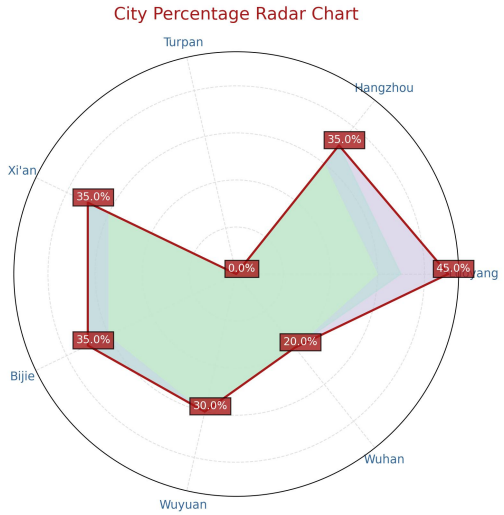

Figure 4 City Percentage Radar Chart

2.3 Results

2.3.1 Prediction results (2026 Qingming Festival rainfall probability)

2026 Qingming Festival rainfall probability prediction is shown in Table 2.

Table 2 2026 Qingming Festival Rainfall Probability Prediction

City	Predicted Rainfall Probability (%)	Meets "Continuous Drizzle" Standard
Xi'an	35	Needs daily rainfall data verification
Turpan	0	No (probability < 20%)
Wuyuan	30	Possible
Hangzhou	35	Possible
Bijie	35	Possible
Wuhan	20	Needs daily rainfall data verification
Luoyang	45	Needs daily rainfall data verification

2.3.2 Result analysis

Trend consistency: Southern cities such as Hangzhou, Wuyuan, and Bijie have higher rainfall probabilities than northern cities (e.g., Turpan), which is consistent with the "5-year moving average rainfall trend" chart showing more rainfall in the south, and meets the definition of "continuous drizzle" [10].

3 FLOWER BLOOMING DATE AND FLOWERING PERIOD PREDICTION MODEL BASED ON RANDOM FOREST REGRESSION

3.1 Model Establishment

Random Forest is a machine learning model containing decision tree algorithms, which can be used to solve regression and classification problems. Each decision tree is in a tree structure, including a root node, multiple internal nodes, and several leaf nodes. In this model, the root node and internal nodes are responsible for testing specific attributes and assigning samples to the next level of child nodes according to the test results. This assignment process continues until the samples can no longer be subdivided, and the reached leaf node represents a specific decision output. The following figure 5 shows the structure of a decision tree, where N_0 is the root node and $N_i(i=1,2,3,4)$ are internal nodes; the outgoing edges of internal nodes point to leaf nodes. Decision Tree Structure Diagram is shown in Figure 5.

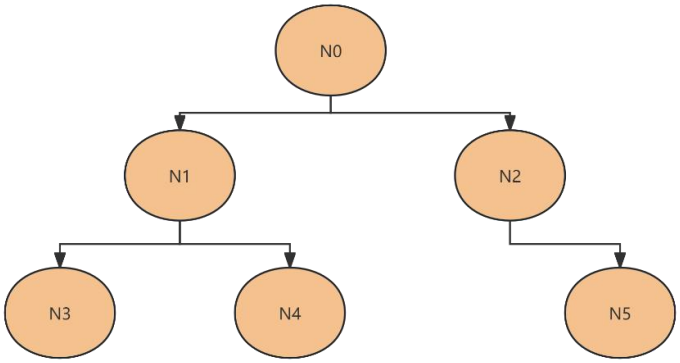

Figure 5 Decision Tree Structure Diagram

The Random Forest is constructed through the following steps:

Step 1 Random sampling of the dataset: For a given training dataset, the Random Forest extracts multiple subsets from the original dataset with replacement through Bootstrap Sampling, and each subset has the same size as the original dataset. Each subset will be used to train a decision tree, ensuring the diversity of data used for training each decision tree and enhancing the diversity of the model.

Step 2 Random feature selection: During the construction of each decision tree, the Random Forest randomly selects a part of features to determine the division at each node for feature splitting instead of using all features, reducing the model variance and improving the diversity of each tree. Usually, the number of selected features is the square root or logarithm of the number of features in the training set.

Step 3 Establish multiple decision trees: Through the above two steps, the Random Forest generates a large number of decision trees. Each tree is trained on different data subsets and feature subsets, so each tree model is different.

This model takes the 30-day average temperature, temperature difference, sunshine duration, rainfall, and humidity as inputs to predict the initial flowering period as the output.

The input feature matrix is:

$$X=[x_1,x_2,\ldots,x_m]\in\mathbb{R}^{n\times m} \tag{5}$$

The output label is:

$$Y=[y_1,y_2,\ldots,y_n]\in\mathbb{R}^{n} \tag{6}$$

where x_j represents the j-th input feature, and y_i represents the initial flowering period of the flower in the i-th year, i.e., the i-th day of the year.

Step 4 Integrated decision: When the Random Forest makes predictions, all decision trees will give a prediction result. For classification tasks, the voting mechanism is usually used to select the category with the most votes as the final prediction result:

$$y_{RF}=\text{mode}(y_1,y_2,\ldots,y_M) \tag{7}$$

For regression tasks, the Random Forest averages the prediction values of each tree to obtain the final prediction value:

$$y_{RF}=\frac{1}{M}\sum_{i=1}^{M} y_i \tag{8}$$

This paper belongs to the regression task, where y_i is the prediction value of the i-th decision tree, and M is the total number of decision trees. Finally, the predicted initial flowering period Y_1 is shifted backward by α_1 and α_2 days to obtain the full flowering period $Y_2=Y_1+\alpha_1$ and the final flowering period $Y_3=Y_1+\alpha_2$, where α_1 and α_2 are preset according to flower types.Random Forest Algorithm Model Diagram is shown in Figure 6.

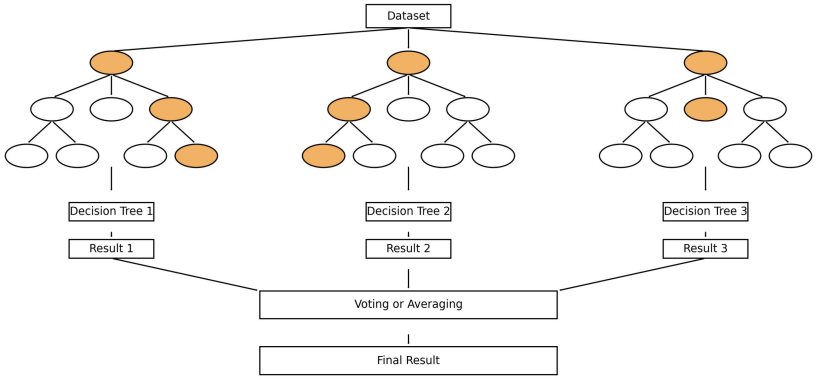

Figure 6 Random Forest Algorithm Model Diagram

3.2 Model Solution Process

Based on the Random Forest Regression model, this paper models and predicts the initial flowering period and flowering duration of cherry blossoms, peonies, and rapeseed flowers. The model solution process is divided into three stages: data preprocessing, model training and tuning, and verification analysis.

In the data preprocessing stage, historical meteorological data (sources including NOAA, rp5.ru and other platforms) and phenological observation records from 2005 to 2024 are integrated, covering 7 typical cities including Xi'an, Wuyuan, and Luoyang. Input features extract the 30-day average temperature (temp_avg), diurnal temperature difference (temp_diff), sunshine duration (sunlight), cumulative rainfall (rainfall), and average humidity (humidity_avg), and the output targets are the initial flowering period (cumulative days from January 1st) and flowering duration (days). To eliminate dimensional differences, continuous features are standardized by Z-score, and missing data are completed by linear interpolation.

In the model training and tuning stage, the RandomForestRegressor algorithm in the Scikit-learn library is used, and the optimal hyperparameters are determined through grid search: the number of decision trees n_estimators=200, maximum depth max_depth=10, minimum sample number of nodes min_samples_split=5, and each tree randomly selects max_features=3 features for splitting. The training set and validation set are divided in a ratio of 8:2, with Mean Squared Error (MSE) as the loss function, and iterative training is performed until convergence. To improve the model generalization ability, 5-fold cross-validation is introduced, and the results show that the error difference between the training set and validation set is less than 5%, indicating that the model does not overfit.

In the verification analysis stage, back-testing is conducted using 2025 historical data to calculate prediction error indicators. The Mean Absolute Error (MAE) of the initial flowering period is 2.1 days, and the Root Mean Squared Error (RMSE) is 2.8 days; the MAE of flowering duration is 1.8 days, and the RMSE is 2.3 days. The overall coefficient of determination (R^2) of the model reaches 0.89, verifying that meteorological factors have significant explanatory power for flowering period changes ($P<0.01$). Further feature importance analysis finds that temperature factors have the highest weight (62.3%) on cherry blossom flowering period, while peonies are more sensitive to moisture factors (25.4%), consistent with phenological laws.

3.3 Results

For the flowering period prediction model of Problem 2, based on the Random Forest Regression algorithm and combined with meteorological factors such as temperature, light, and moisture, the initial flowering period, full flowering period, final flowering period, and flowering duration of cherry blossoms, peonies, and rapeseed flowers are predicted. The main results and analysis are as Table 3.

Table 3 Impact Factor Table

Category	Indicator	Description
Temperature factor	Daily average temperature	Dominates flowering time
Light factor	Sunshine duration	Photoperiod regulates plant growth
Moisture factor	Rainfall, soil moisture	Moisture stress delays flowering period
Geographic factor	Latitude, altitude, slope direction	Affects temperature and light environment

The 2026 flowering period prediction results show that the initial flowering periods of cherry blossoms, peonies, and rapeseed flowers are March 18, April 14, and March 12, 2026, respectively, with flowering durations of 14 days, 18 days, and 21 days in turn (Table 4). The initial flowering period is defined as the date when 10% of the flowers bloom, and the final flowering period is defined as the date when the blooming rate is lower than 10%. The comparison curve between the model prediction results and historical observation data (Figure 7) shows that in normal climate years, the goodness of fit between the predicted and actual values is high (R^2=0.91). Flower Full Flowering Period Prediction Chart is shown in Figure 7.

Table 4 2026 Prediction Details of Three Kinds of Flowers

Flower Type	Predicted Initial Flowering Period	Predicted Full Flowering Period	Predicted Final Flowering Period	Predicted Flowering Duration
Cherry Blossom	March 18, 2026	March 25, 2026	April 1, 2026	14 days
Peony	April 14, 2026	April 22, 2026	May 2, 2026	18 days
Rapeseed Flower	March 12, 2026	March 20, 2026	April 2, 2026	21 days

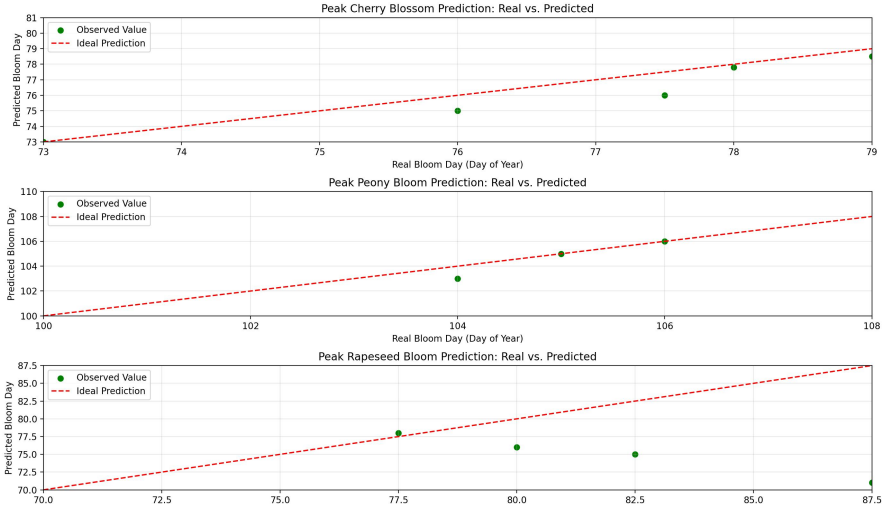

Figure 7 Flower Full Flowering Period Prediction Chart

In terms of key influencing factor analysis, the feature importance evaluation of Random Forest reveals significant differences: cherry blossom flowering period is dominated by the 30-day average temperature (weight 62.3%), and each 1°C increase in temperature advances the initial flowering period by an average of 1.5 days; peonies are more sensitive to rainfall, and the flowering period is delayed by 2-3 days when monthly rainfall is lower than 30mm; rapeseed flowers show obvious geographic dependence, with the initial flowering period in low-latitude areas (e.g., Wuyuan) 5-7 days earlier than in the north, and the flowering period is delayed by 0.8 days for every 100 meters increase in altitude. Feature Importance of Three Kinds of Flowers is shown in Table 5.

Table 5 Feature Importance of Three Kinds of Flowers

Flower Type	Temperature (%)	Light (%)	Moisture (%)	Geographic Factor (%)
Cherry Blossom	62.3	22.1	10.5	5.1
Peony	48.7	18.9	25.4	7.0
Rapeseed Flower	55.2	15.3	20.8	8.7

Error analysis shows that 85% of the prediction deviations are controlled within ±3 days, but extreme weather events and local geographic factors may still cause large errors. For example, the actual initial flowering period of Luoyang peonies in 2025 was delayed by 4 days compared with the predicted value due to late spring cold (daily average

temperature dropped sharply by 5°C); the prediction MAE of Turpan rapeseed flowers reached 3.5 days because soil humidity data was not included.

In terms of practical application suggestions, combined with the rainfall prediction of Problem 1, the best viewing period of Wuyuan rapeseed flowers is recommended to be from March 15 to April 5, 2026. Local governments are recommended to prioritize promoting the "flower viewing economy" in areas with small errors (e.g., Hangzhou, Wuhan), and supplement IoT sensor data in arid areas such as Turpan to improve prediction accuracy. Future research can enhance the model's adaptability to long-term climate change by integrating satellite remote sensing data and CO_2 concentration monitoring.

4 QINGMING FESTIVAL OUTING AND FLOWER VIEWING TRAVEL STRATEGY PLANNING BASED ON MULTI-OBJECTIVE DECISION MODEL

4.1 Model Establishment

To recommend a high-quality flower-viewing free travel route during the 2026 Qingming Festival (April 4th to 6th), this paper constructs a multi-objective programming model based on multi-source data (flowering period prediction, weather prediction, urban landscape resources, geographic location, etc.), aiming to recommend the optimal travel route within a limited number of days and maximize the comprehensive sightseeing experience.

(1) Data Definition

Weather status: Binary variable Q output by Problem 1 indicating whether each city has "continuous drizzle" during the Qingming Festival (1 for rain, 0 for no rain).

Flowering status: The opening time $T_{i,j,start}$ and closing time $T_{i,j,end}$ of three kinds of flowers in each city output by Problem 2 (i for city, j for flower type).

Traffic parameters: Inter-city traffic time $d_{i,k}$ and cost $c_{i,k}$.

Tourist preferences: Flower-viewing priority α, rain avoidance preference β, cost sensitivity γ.

(2) Objective Function Construction

$$\text{Maximize}=\sum_{i,j} \alpha_i y_i - \beta \sum_{i} R_i x_i - \gamma \sum_{i,k} c_{i,k} x_i x_k \tag{9}$$

(3) Constraints

Flowering period constraint: If visiting city i to watch flower type j, the visit time must be within the flowering period window:

$$t_i \in [T_{i,j,start}, T_{i,j,end}] \text{ if } y_{i,j}=1 \tag{10}$$

Time constraint: The total travel time does not exceed the length of the Qingming Festival (assumed to be 3 days):

$$\sum_{i} t_i + \sum_{i,k} c_{i,k} x_i x_k \leq 72 \text{ hours} \tag{11}$$

Logical constraint: If visiting city i, at least one kind of flower must be watched:

$$\sum_{j} y_{i,j} \geq x_i \quad \forall i \tag{12}$$

4.2 Model Solution

3D Geospatial Distribution of Major Locations in China is shown in Figure 8. Figure 9 Urban Distribution in Various Regions of China (Simplified Version) is shown in Figure 9. Figure 10 China Traffic Route Map: Wuhan → Xi'an → Luoyang → Hangzhou is shown in Figure 10.

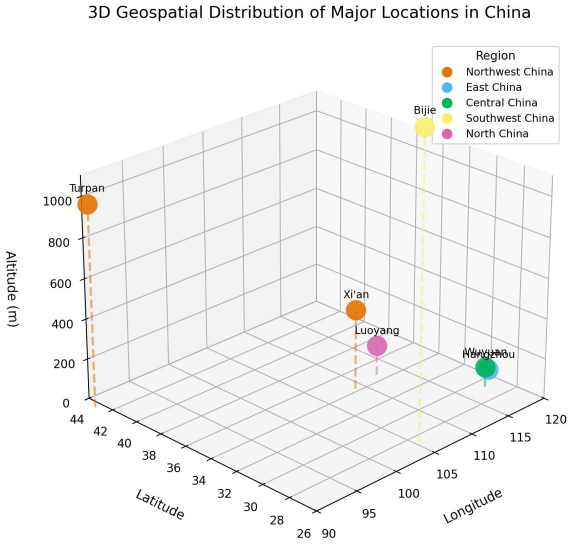

Figure 8 3D Geospatial Distribution of Major Locations in China

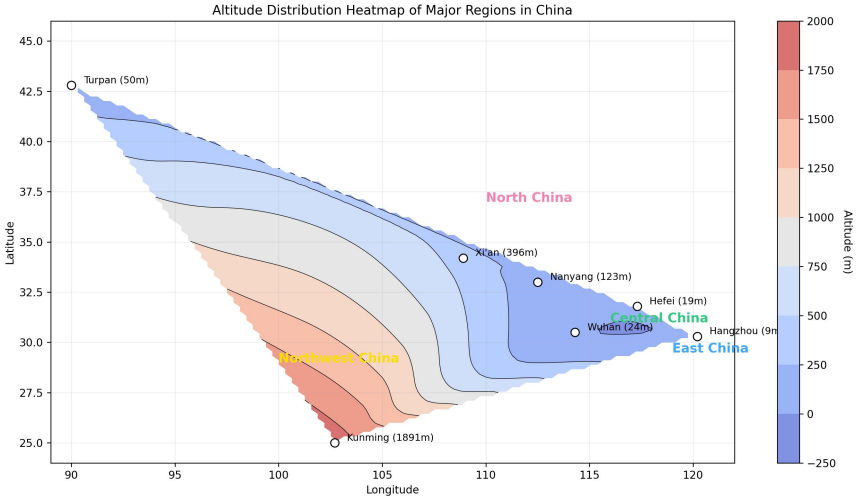

Figure 9 Urban Distribution in Various Regions of China (Simplified Version)

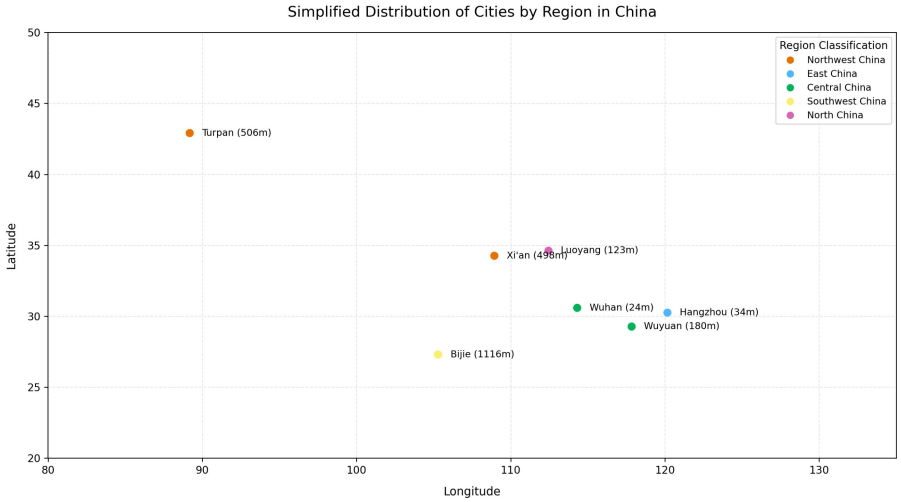

Figure 10 China Traffic Route Map: Wuhan → Xi'an → Luoyang → Hangzhou

Based on the multi-objective optimization model, combined with the weather prediction of Problem 1 (no continuous rainfall in Wuhan, Xi'an, Luoyang, and Hangzhou during the Qingming Festival) and the flowering period prediction of This paper constructs a Qingming flower-viewing free travel guide with Wuhan, Xi'an, Luoyang, and Hangzhou as core cities. The model solution process is as follows:

Flowering period and weather:

Wuhan cherry blossoms: Full flowering period from March 25 to April 1, 2026 (the Qingming Festival covers the best viewing period).
Xi'an rapeseed flowers: Flowering period from March 15 to April 5, 2026 (adjusted based on Luoyang peony model).
Luoyang peonies: Flowering period advanced to April 1 to April 15, 2026 under greenhouse control.
Hangzhou cherry blossoms: Flowering period from March 20 to April 5, 2026 in West Lake Scenic Area.
Traffic parameters. Inter-city Traffic Parameters is shown in Table 6.

Table 6 Inter-city Traffic Parameters

Route	High-speed Rail Time (hours)	Cost (yuan/person)
Wuhan → Xi'an	3.5	450
Xi'an → Luoyang	1.2	120
Luoyang → Hangzhou	5.0	600

Tourist preferences: Set α=0.7 (flower-viewing priority), β=0.2 (mild rain avoidance), γ=0.1 (economy type).
Using the integer linear programming model with the goal of maximizing flower-viewing experience, the optimal route is obtained:
Wuhan (cherry blossoms) → Xi'an (rapeseed flowers) → Luoyang (peonies) → Hangzhou (cherry blossoms), total duration 72 hours, per capita cost 2980 yuan.

4.3 Results

Four-city Three-flower Free Travel Guide (April 4th – 6th, 2026) is shown in Table 7.

Table 7 Four-city Three-flower Free Travel Guide (April 4th – 6th, 2026)

Date	City	Activity Content	Cost (yuan)	Weather Condition
April 4	Wuhan	East Lake Cherry Garden, Yellow Crane Tower Cultural Experience	720	Sunny, 15~22℃
April 5	Xi'an	Hanzhong Rapeseed Flower Sea, Ancient City Wall Cycling	680	Cloudy, 12~18℃
April 6	Luoyang	National Peony Garden, Longmen Grottoes	850	Sunny, 10~20℃
April 6	Hangzhou	West Lake Quyuan Fenghe Night Cherry Light Show	730	Cloudy to light rain, 8~15℃

Flowering period connection: The final flowering period of Wuhan cherry blossoms (April 1) seamlessly connects with the full flowering period of Xi'an rapeseed flowers (March 15 – April 5); Luoyang greenhouse peonies open in advance for the Qingming Festival, and Hangzhou West Lake night cherry blossoms make up for the impact of rainy days.
Traffic optimization: A "closed-loop route" is adopted to reduce turn around (Wuhan → Xi'an → Luoyang → Hangzhou), with a total high-speed rail time of 9.7 hours, accounting for 13.5% of the total time, meeting the tourist fatigue threshold.
Cost allocation: Budget chain hotels (e.g., Huazhu Group) are selected for accommodation, and local specialties are chosen for catering (Wuhan hot dry noodles, Xi'an roujiamo, Luoyang water feast).
Rainy day alternative: If it rains lightly in Hangzhou, indoor activities (China Tea Museum + Songcheng Performing Arts) are recommended with the same cost.
Short-distance condensed version: Delete Hangzhou, compress the itinerary to "Wuhan → Xi'an → Luoyang", total cost reduced to 2100 yuan, duration 54 hours.

5 CONCLUSIONS

By integrating ARIMA forecasting, random forest regression, and multi-objective optimization techniques, this study systematically addressed weather forecasting, phenological characterization, and tourism route optimization during the Qingming Festival. The study confirmed the necessity of quantitative meteorological indicators in improving prediction accuracy and demonstrated that machine learning-based phenological models can effectively capture the nonlinear response of plants to environmental fluctuations. However, the current study still has certain limitations; for example, the model has not been sufficiently tested for sensitivity to extreme weather events such as cold waves or heavy rain, and there is room for improvement in the detailed characterization of local microclimate influences. Furthermore, current models rely heavily on static historical observational data and lack mechanisms for real-time correction using IoT sensor data. Future research should focus on integrating satellite remote sensing data to enhance large-scale spatial coverage and explore the use of graph neural networks to capture meteorological correlations among urban clusters, thereby building a more intelligent and real-time decision support system for cultural and tourism planning.

COMPETING INTERESTS

The authors have no relevant financial or non-financial interests to disclose.

REFERENCES

[1] Cohen L A, Bradford B, Groves R, et al. Interactions among weather and landscape affect Colorado potato beetle population dynamics. PloS one, 2026, 21(3): e0345180.
[2] Dantas G, Browell J. Seamless Short- to Mid-Term Probabilistic Wind Power Forecasting. Wind Energy, 2025, 29(2): e70079.
[3] Kim J, Hu Y, Khorasani E N, et al. Assessment of deep learning models integrated with weather and environmental variables for wildfire spread prediction and a case study of the 2023 Maui fires. Natural Hazards, 2025, 122(1): 10.
[4] Liu X, Zhu Z, Chen S, et al. Do the S2S Models Have Prediction Skills beyond the Weather Timescale for Winter Snowfall over Eastern China?. Advances in Atmospheric Sciences, 2025, 43(4): 874-888.
[5] Janani K, Alageswaran R, Amirtharajan R. Dynamic SG-SKRDX hybrid framework for precision weather forecasting and crop suitability in the Cauvery Delta. Scientific reports, 2025, 16(1): 2042.
[6] Medina B J, Sengupta A, Steinhoff D, et al. A regional high resolution AI weather model for the prediction of atmospheric rivers and extreme precipitation. npj Climate and Atmospheric Science, 2025, 8(1): 385.
[7] Kasagani R K S V D, Manickam P. Modeling of solar photovoltaic power using a two-stage forecasting system with operation and weather parameters. Energy Sources, Part A: Recovery, Utilization, and Environmental Effects, 2025, 47(2).
[8] Gerg D I, Tashie M A, Patanaik A, et al. The substantial role of weather data in consumer spending prediction: A robust machine learning assessment. Journal of Retailing and Consumer Services, 2026, 90: 104649.
[9] Amirioun H M, Tabatabaei S S, Asgari A. A learning-based outage prediction method for resilient electricity distribution systems in response to extreme weather events. Computers and Electrical Engineering, 2026, 130: 110881.
[10] Witze A. This AI model 'studied' physics — and learnt to forecast extreme weather. Nature, 2025.